Fast Magnetic Reconnection Processes

F. Brunel and T. Tajima
Institute for Fusion Studies, The University of Texas at Austin, Austin, Texas 78712

and

J. M. Dawson
Department of Physics, University of California, Los Angeles, Los Angeles, California 90024

(Received 13 October 1981)

It is found through theory and magnetohydrodynamic particle simulation that fast magnetic-field-line reconnection may consist of more than one stage. After the Sweet-Parker phase is established for an Alvén time, a faster "second phase" of reconnection takes over if the plasma is compressible: The reconnected flux varies as $\psi = \psi_0 t^{\rho_i/\rho_e}$, where ρ_e and ρ_i refer to the plasma densities outside and inside of the current channel.

PACS numbers: 52.30.+r, 52.35.Mw, 52.55.Ez, 52.65.+z

Fast magnetic-field-line reconnection is a prerequisite to formation of a compact plasma toroid.[1-4] This process was observed in the simulation of a reversed theta pinch at the island stage, but also at the island destruction stage once the tilting instability set in.[5] A fast reconnection process is again responsible for destruction of the reversed z pinch[6] as well as for Kadomtsev's model[7,8] of tokamak disruption. Rapid reconnection is also believed to play an important role in the magnetosphere, the sun's dynamo, etc. From our studies by magnetohydrodynamic (MHD) particle simulation and subsequent theoretical development, we have found some general characteristics of nonlinear evolution of fast reconnection and we report, in particular, the discovery of multiple phases for this process.

Computer simulation has been carried out on a $2\frac{1}{2}$-dimensional MHD particle code[9] with the Lax-Wendroff algorithm to advance the magnetic field. Initially, homogeneous magnetic fields in the x direction are embedded in a plasma with opposite senses in the lower and upper halves. In order to make the physics simpler, we let the layer between the two regions with reversed fields (i.e., $|y| \leq a$) contain a high-density uniform plasma and no magnetic field, and have sharp boundaries. (Similar results have been obtained with smooth boundaries.) The system is periodic in x and is bounded in the y direction by perfect conductors, and the perpendicular pressure equilibrium is satisfied until we pinch the plasma locally by one (or two) external current rod(s) normal to the x-y plane (in the z direction). Figure 1(a) shows an early stage of the magnetic fields pinched by one rod.

As the external current pinches the plasma, the magnetic field lines as well as the high-density plasma slab are pinched downward [Fig. 1(a)]. The perpendicular pressure balance is increased in the region close to the current rod and becomes nonuniform along the column. Since the pressure is not balanced in the parallel direction, the plasma in the layer is drawn away from the region of the rod along the field lines. As the plasma flows out, the thickness of the layer decreases exponentially in time,[10] while the local density in the layer remains high. In ideal MHD, the plasma layer develops into a singular current sheet, in a quasistationary state, always out of equilibrium.[11]

For resistive (or nonideal MHD) plasmas, however, the layer width becomes stabilized as field lines begin reconnecting at such a rate that the perpendicular inflow of particles into the current sheet due to the field-line annihilation matches the plasma end loss along the magnetic field lines [see Fig. 1(c)] due to the parallel pressure drop. The inflow is governed by magnetic diffusion due to resistivity in the layer. This is a slow process (although certainly faster than the Rutherford process in the equilibrium) described earlier by Sweet and Parker.[12] We quantify this process by the succeeding analysis.

The in-the-plane magnetic flux ψ and out-of-the-plane (along the z axis) magnetic field B_z are described by

$$\partial\psi/\partial t + \vec{v}\cdot\nabla\psi = \eta\nabla^2\psi, \tag{1}$$

$$\partial B_z/\partial t + \nabla\cdot\vec{v}B_z = \eta\nabla^2 B_z, \tag{2}$$

where $\vec{B} = \vec{B}_\perp + B_z\vec{e}_z$ and $\vec{B}_\perp = \nabla\psi\times\vec{e}_z$; v_z is neglected. For the initial configuration we assume the flux function to be linearly increasing in y, $\psi = B_e|y|$, on each side of the exteriors of the current sheet located at $y = 0$; this is equivalent to

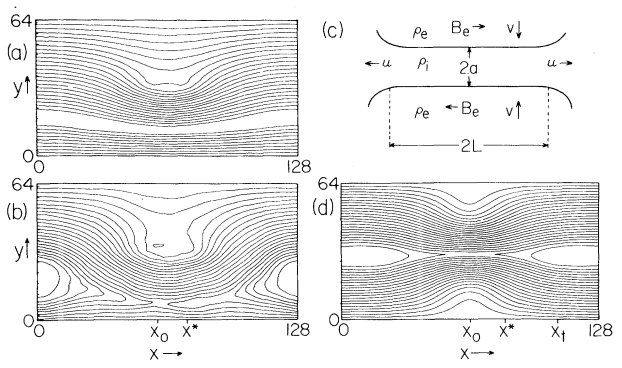

FIG. 1. Flux lines ψ. One-pinch case in (a) the Sweet-Parker phase ($t = 30$) and (b) the second phase ($t = 75$), where L^* is indicated ($L^* = x^* - x_0$). (c) Sweet and Parker model for reconnection. (d) Two-pinch case in the second phase ($t = 75$), where L^* and L_t ($L_t = x_t - x_0$) are shown. t is in units of Δ/c_s, where Δ is the grid spacing in y and c_s is the sound speed.

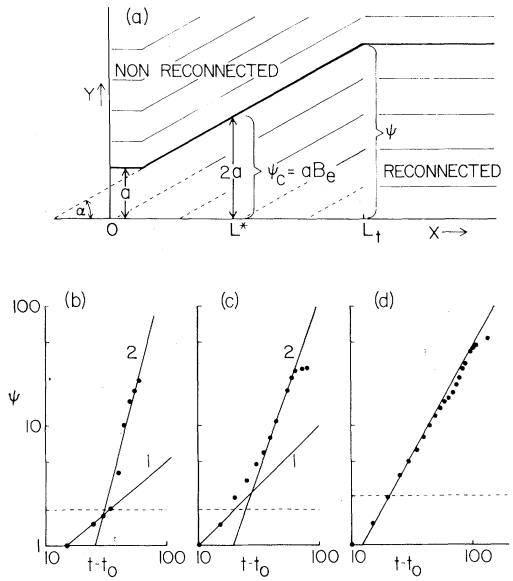

FIG. 2. (a) Model for the "second phase." (b)–(d) log-log plots of ψ vs t. (b) One-pinch case with resistivity $\eta = 0.01$. Line 1 has a slope 0.86 and line 2 has 4.0. (c) One-pinch case with $\eta = 0.1$. Line 1 has slope 1.0 and line 2 has 2.9. (d) Two-pinch case $\eta = 0.1$ with slope 1.8 in units of $c_s\Delta$. We have defined $x^* = x_0 + L^*$ and $x_t = x_0 + L_t$.

the assumption of a uniform magnetic field of magnitude B_e, but as shown in Fig. 1(c). In these exterior regions the diffusion terms are negligible and the flux velocity is determined by the fluid in the y direction:

$$v = \dot{\psi}/B_e. \tag{3}$$

Inside of the current sheet with half-width a, the perpendicular velocity v is zero and the diffusion process becomes important:

$$\dot{\psi} = \eta\nabla^2\psi \simeq \eta B_e/a. \tag{4}$$

The balance of the perpendicular inflow with the longitudinal outflow gives

$$\rho_e v L = \rho_i u a, \tag{5}$$

where subscripts e and i refer to the external and internal quantities with respect to the current sheet. Equations (3) and (5) give

$$\dot{\psi} = B_e u \rho_i a/\rho_e L, \tag{6}$$

while Eqs. (4) and (5) yield

$$a = \eta^{1/2}(\rho_e L/\rho_i u)^{1/2}. \tag{7}$$

The peak density ρ_i with respect to ρ_e is determined by the perpendicular pressure balance $p_i + B_{iz}^2/8\pi = p_e + B_{ez}^2/8\pi + B_{e\perp}^2/8\pi$ and we use an adiabatic law for p, i.e., $p/\rho^\gamma = \text{const}$. The plasma slab develops a diffuse profile as it becomes thinner as shown by Eq. (4). Thus ρ_i in Eq. (5) and thereafter is the average density over the slab cross section (which is about 60% to 80% of the original peak value). The flow velocity u is determined by the drop in perpendicular pressure $B_\perp^2/8\pi$ along x,[10] and is $c_{Ae}(\rho_e/\rho_i)^{1/2}$ (when $B_\perp$ can be neglected at the cusp). This gives

$$v = R_m^{-1/2} c_{Ae}(\rho_i/\rho_e)^{1/2}, \tag{8}$$

where the magnetic Reynolds number $R_m = c_{Ae}L/\eta$ and the Alfvén velocity $c_{Ae} = (B_{\perp e}^2/4\pi\rho_e)^{1/2}$. Sweet and Parker[12] gave an incompressible version ($\rho_i = \rho_e$) of Eq. (8).

If the plasma is compressible, however, the poloidal flux reconnected in the Sweet-Parker phase may pile up in the current sheet as time goes on. The current sheet then becomes tapered, shortening the effective exhaust distance L. It is at this stage when a drastic enhancement in the reconnection rate is observed in our simulation [see Fig. 1(b)]. A simplified model of this stage may be depicted as in Fig. 2(a). The trapped reconnected flux has a tapered structure with pitch angle α, where α is small enough compared with unity that the initial pressure balance and, therefore, ρ_i/ρ_e, are not modified significantly. As a new flux tube reconnects at $x = 0$, its plasma pressure goes up to P_i (we define $P = p + B_z^2/8\pi$) over width a. However, at distance $L^* = a/\alpha$ along the x axis, this flux tube is located at $a < y$

$< 2a$ outside the diffusive area, with a magnetic field B_e and a plasma pressure P_e. Since no magnetic pressure gradient exists along the field line (with angle α from the x axis), at $x = L^*$ the parallel pressure satisfies $\rho_i u^2/2 = P_i - P_e$. Therefore, the plasma in that flux tube will flow with a velocity $u = c_A(\rho_i/\rho_e)^{1/2}$ (Ref. 10) along the α direction. The angle α is determined by $\alpha = B_y/B_e$ [see Fig. 2(a)], where B_y is the average magnetic field along y in the diffusion layer, given by $B_y = \psi/L_t$, where ψ is the total reconnected flux and L_t the length along the x direction traveled by flux ψ. With $L_t = L^* + ut$, we obtain

$$L^* = ut\psi_c/(\psi - \psi_c), \tag{9}$$

where $\psi_c \equiv aB_e$. In the evaluation of L_t we assume that the flux in the current sheet is carried instantly over a distance L^* where diffusion is predominant, and then remains trapped with the fluid which moves with a velocity u along x. Once L^* becomes shorter than L, which happens when $\psi > \psi_c$ or $t > t_0 \simeq L/u$, substitution of Eq. (9) into Eq. (6) yields $t\dot{\psi} - (\rho_i/\rho_e)\psi = -\psi_c$ or

$$\psi = \psi_0(t/t_0)^{\rho_i/\rho_e} + (\rho_e/\rho_i)\psi_c. \tag{10}$$

If the plasma is compressible, the reconnection rate becomes much faster than that in the Sweet-Parker phase after t_0 with a shrinking current sheet L^*. There will be a sharp increase in the reconnection velocity given by $v = \dot{\psi}/B_e \propto t^{\delta}$, with $\delta = \rho_i/\rho_e - 1$. We shall call this stage of faster reconnection the *second phase*. If the plasma is incompressible ($\rho_i = \rho_e$), the Sweet-Parker phase lasts beyond t_0. Correspondence to relations in Eqs. (9) and (10) can be found in our simulation in Figs. 1(a) and 1(b) for shrinking L^* and in Figs. 2(b) and 2(c) for two (or more) phases of $\psi(t)$. The exponent obtained from Fig. 2(b) for the second phase is 4.0 with $\rho_i/\rho_e \simeq 4.0$ in the simulation, and the exponent from Fig. 2(c) is 2.9 with $\rho_i/\rho_e \simeq 3.4$; both cases are in good agreement with Eq. (10).

The magnetic force that pulls the plasma out of the current sheet in the x direction contains two terms: one is similar to $\alpha^2 B_e^2/8\pi a$ due to the curvature of B_y and the other is the x component of the perpendicular magnetic pressure $F_m = \alpha B_e^2/8\pi\tilde{a}$ considered by Petschek,[13] where $\tilde{a}(x)$ is the local column width. The latter is much larger than the former and is of the same order of magnitude as the parallel plasma pressure drop F_p considered here. Because $\alpha = a/L^*$ and $B_e^2/8\pi = P_i - P_e$, the term F_m is about $(a/\tilde{a})F_p$, and it is large for $|x| < L^*$ where $\tilde{a} \simeq a$. It is noted, however, in our simulation that the plasma in the reconnected region flows along the field lines as assumed by us, and takes a tapered shape with angle α. The Petschek term F_m is, therefore, largely canceled by the pressure term $\alpha(P_i - P_e)/\tilde{a}$.

The geometry of the system is important both for the second phase and for the eventual saturation of reconnection. When the current layer is pinched from both sides so that it remains straight during the reconnection process, a different exponent for the time dependence for the reconnected flux is observed in the second phase. Figure 1(d) shows the flux lines in this case. The rate of reconnection in this case is given in Fig. 2(d): $\psi \simeq (t - t_0)^{\xi}$ where $\xi \simeq 2$.

In this latter case we propose the following mechanism which impedes the process in Eq. (10). In slab geometry field lines due to the combination of a dipole (B_d on axis) and uniform B_e are approximately described by

$$y(x) = y_0(1 + \theta x^2/r_d^2), \tag{11}$$

where $|y| \ll r_d$ (close to the plane of symmetry). Here $\theta = B_d/(B_d + B_e)$ and $2r_d$ is the dipole distance. In this geometry the flux is packed in such a way that the reconnected flux $\psi \leq B_e y(x)$ with $x = L_t \sim ut$, where the field line $y(0) = a$ is considered. Using these conditions in Eq. (11), we obtain

$$\psi \simeq aB_e\theta(ut)^2/r_d^2. \tag{12}$$

If $\psi > B_e y(x)$, the field line would be pushed away, increasing the current sheet thickness and therefore stopping the diffusion and reconnection process. The reason this process in Eq. (12) is slower than Eq. (10) is that when we pinch from both sides, the reconnected field lines close to the current sheet (which is the plane of symmetry for this case) stay straighter and open up less angle. Equation (12) agrees well with simulation results [Fig. 2(d)].

Finally, previous simulation investigations are consistent with our theory and simulation. Sato and Hayashi's simulation[14] (their Fig. 1) shows that fast reconnection sets in when L^* becomes the length of their system, consistent with the present theory of the second phase. Park's work[8] notes that the incompressible case stays in the Sweet-Parker phase all the way. In the island coalescence process, this second phase of fast coalescence should also exist in the small-η case described by Biskamp and Welter[15] if the plasma is compressible. Our particular model is one of many[5-8,14,15] which give rise to a current singu-

larity. (It corresponds to the setup in Ref. 5 to initiate island formation in a reversed pinch.) However, the model and its subsequent physics are general enough to pertain to many other cases, since nonlinear developments are common over many situations, e.g., the external driven pinch reconnection, the development of the internal coalescence instability, etc.

This work was supported by the U. S. Department of Energy Grant No. DE-5G05-80ET-53088 and by the National Science Foundation Grants No. PHY80-26048 and No. ATM81-10539.

[1]H. Alfvén, L. Lindberg, and P. Mitlid, J. Nucl. Energy, Part C 1, 116 (1960).
[2]J. H. Irby, J. F. Drake, and H. R. Griem, Phys. Rev. Lett. 42, 228 (1979).
[3]T. R. Jarboe, I. Henins, H. W. Hoida, R. K. Linford, J. Marshall, D. A. Platts, and A. R. Sherwood, Phys. Rev. Lett. 45, 1264 (1980).
[4]W. C. Turner *et al.*, Lawrence Livermore Laboratory Report No. UCRL-85122, 1980 (unpublished).
[5]F. Brunel and T. Tajima, Bull. Am. Phys. Soc. 25, 884 (1980).
[6]E. J. Caramana and D. D. Schnack, in Proceedings of the 1981 Sherwood Theory Meeting (unpublished), Paper No. 3B38.
[7]B. B. Kadomtsev, Fiz. Plazmy 1, 710 (1975) [Sov. J. Plasma Phys. 1, 389 (1975)].
[8]W. Park, Bull. Am. Phys. Soc. 26, 845 (1981).
[9]F. Brunel, J. N. Leboeuf, T. Tajima, J. M. Dawson, M. Makino, and T. Kamimura, J. Comput. Phys. 43, 268 (1981).
[10]F. Brunel, T. Tajima, J. N. Leboeuf, and J. M. Dawson, Phys. Rev. Lett. 44, 1494 (1980).
[11]S. I. Syrovatskii, Zh. Eksp. Teor. Fiz. 60, 1727 (1971) [Sov. Phys. JETP 33, 933 (1971)].
[12]E. N. Parker, Astrophys. J. Suppl. Ser. 77, 177 (1963).
[13]H. E. Petschek, in *Symposium on the Physics of Solar Flares*, edited by W. N. Hess (NASA, Washington, D.C., 1964), p. 425.
[14]T. Sato and T. Hayashi, Phys. Fluids 22, 1189 (1979).
[15]D. Biskamp and H. Welter, Phys. Rev. Lett. 44, 1069 (1980).

Ion Heating with High-Power Perpendicular Neutral-Beam Injection in the Poloidal Divertor Experiment (PDX)

R. J. Hawryluk, V. Arunasalam, M. Bell, M. Bitter, K. Bol, K. Brau, S. Davis, F. Dylla, H. Eubank, M. Finkenthal, R. Fonck, R. Goldston, B. Grek, J. Hugill,[a] D. Johnson, R. Kaita, S. Kaye, H. Kugel, D. Mansfield, D. Manos, K. McGuire, R. McCann, D. McCune, D. Mueller, M. Okabayashi, K. Owens, M. Reusch, N. Sauthoff, G. Schilling, G. Schmidt, S. Sesnic,[b] S. Suckewer, G. Tait, H. Takahashi, F. Tenney, and K. Yamazaki[c]

Princeton University Plasma Physics Laboratory, Princeton, New Jersey 08544
(Received 10 February 1982)

Plasma heating by near-perpendicular injection of up to 7.2 MW of neutral-beam power has been studied in the PDX tokamak. Collisionless plasmas with central ion temperatures up to 6 keV have been obtained. The total plasma energy, which is dominated by contributions from beam and thermal ions, rises linearly with increasing beam power. The ion heating efficiency in PDX is comparable to that measured in the Princeton Large Torus with tangential injection.

PACS numbers: 52.55.Gb, 52.50.Gj, 52.55.Pi

Neutral beams have been used for auxiliary heating in many tokamak experiments. In most, the beams have been injected essentially tangentially to the toroidal magnetic field. For future large machines, perpendicular injection is attractive for achieving good beam penetration at beam energies that are practical for positive ion sources. Up to ~1 MW was injected near-perpendicularly into the TFR tokamak.[1] On the Poloidal Divertor Experiment (PDX), these results have been extended to power levels of 7.2 MW to examine the effectiveness of perpendicular injection in heating plasmas to the high-temperature, low-collisionality regime which will be typical of the next generation of devices.

The PDX tokamak is described by Meade *et al.*[2]